Diffusion Fundamentals
J. Kärger, P. Heitjans, F. Grinberg, G. Schütz
www.diffusion-fundamentals.org

PFG NMR measurements of tortuosity factors for diffusion in meso- and macropores of FCC catalysts

S. Vasenkov, P. Kortunov

Universität Leipzig, Fakultät für Physik und Geowissenschaften, Linnéstr. 5, D-04103
Leipzig, Germany

(received 4 February 2005, accepted 11 February 2005)

Abstract

Pulsed field gradient (PFG) NMR is applied to measure self-diffusion coefficients of 1,3,5 tri-isopropyl-benzene in the particles of several industrial FCC catalysts having different systems of meso- and macropores. Relating these diffusivities to the self-diffusion coefficient of 1,3,5 tri-isopropyl-benzene in the liquid phase, the tortuosity factors for diffusion in the meso- and macropores of the particles were obtained. The values of the tortuosity factors were found to increase with a increasing volumetric fraction of the small (< 20 nm) meso- and macropores in the total intraparticle volume.

Studies of the diffusion of liquids in random porous systems attract considerable interest because of the importance of this process for numerous industrial applications. In particular, transport of reactant and product molecules in porous catalysts may play an essential role in catalytic reactions. It may even determine the conversion rate and selectivity of catalytic processes when the rate of the supply of reactant molecules to and the rate of the removal of products from the active sites of porous catalysts is controlled by diffusion. This paper focuses on diffusion in fluid catalytic cracking (FCC) catalysts. A typical particle of FCC catalyst possesses a complex system of pores, which include micropores of the zeolite crystals located in the particles and meso- and macropores located in the so-called “matrix”, which surrounds zeolite crystals (Fig.1).

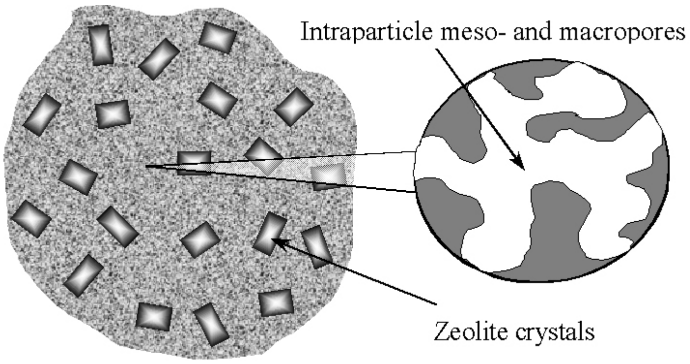

Fig.1 Schematic presentation of a particle of a typical FCC catalyst.

Diffusion under molecular confinement in the micropores of zeolites has been a subject of a large number of recent studies [1-6]. In comparison, significantly smaller effort has been devoted to understanding of the transport in meso- and macropores of various porous catalysts, including FCC catalysts.

Transport properties of random porous systems consisting of meso- and macropores can be characterized in terms of the tortuosity factor. This factor reflects the extent of an increase of the trajectory lengths of the diffusing molecules due to reflections from the pore walls in comparison to the corresponding trajectory lengths in the liquid phase for the same mean square displacements.

Here we report the tortuosity factors for a set of four industrial FCC catalysts, which were fabricated by Grace GmbH, Germany. Each catalyst consists of particles with sizes around 70 μm. The particles of all catalysts have, on average, the same fractions of the same zeolite USY. The mean size of the zeolite crystals, which consist of many intergrown crystallites, was smaller than 1 micron. Different fabrication conditions have been used for different catalysts in order to prepare samples with different systems of meso- and macropores.

The diffusion measurements have been performed by the pulsed field gradient (PFG) NMR technique [1,7,8] using the home-built PFG NMR spectrometer FEGRIS NT operating at a ^{1}H resonance frequency of 400 MHz [9]. The 13-interval bipolar PFG pulse sequence was used [10]. This sequence allows the suppression of distortions of PFG NMR diffusion results by internal magnetic field inhomogeneities (i.e., internal magnetic field gradients) induced by susceptibility variations in heterogeneous samples. 1,3,5 tri-iso-propyl-benzene was chosen as a probe molecule for diffusion measurements. This choice is related to the fact that the molecules of 1,3,5 tri-iso-propyl-benzene are too large to be able to penetrate into the micropores of the zeolite USY [11] located in particles of FCC catalysts. Hence, the diffusion data obtained with these molecules is expected to reflect only the transport properties of the meso- and macropores located in the particles. The samples for the PFG NMR measurements were prepared as follows. Around 300 mg of FCC catalyst were loaded into the NMR tube. Then the tube with the catalyst was connected to the vacuum system. This was followed by the catalyst dehydration under high vacuum at 473 K for 20 hours. After the dehydration, the catalyst sample was cooled down to room temperature and the liquid 1,3,5 tri-iso-propyl-benzene was introduced into the PFG NMR tube. The amount of the liquid adsorbate was chosen in such a way that the catalyst in the tube was completely covered with the liquid. This condition ensures that all intraparticle meso- and macropores are completely filled with the liquid. Upon loading, the NMR tube was sealed and separated from the vacuum system.

Fig.2 shows examples of the measured PFG NMR attenuation curves in the catalyst samples at 297 K. In the case when the diffusion process obeys the laws of normal (i.e. Fickian) diffusion with a single diffusivity, the attenuation curves obtained with the 13-interval sequence can be described by the single-exponential dependence [10]

$$\Psi = \exp\left(-4\gamma^2\delta^2\boldsymbol{g}^2\boldsymbol{Dt}\right), \qquad (1)$$

where g and δ are, respectively, the amplitude and duration of the applied gradient pulses, D denotes the diffusivity, t is the effective diffusion time, and γ is the gyromagnetic ratio. In the presentation of Fig.2 the attenuation curves obeying Eq.1 should look like straight lines. The results presented in Fig.2 obviously show a more complex behavior, which is not unexpected.

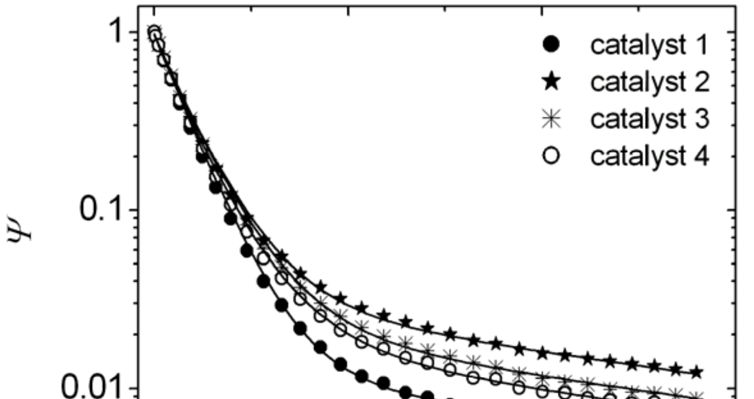

Fig.2 ^{1}H PFG NMR spin echo attenuation curves (points) measured by using the 13-interval PFG NMR sequence for 1,3,5 tri-iso-propyl-benzene in different FCC catalysts containing the same fraction of the same zeolite USY. The diffusion time in all cases was equal to 30 ms. Lines show the best fit of the experimental curves by using Eq.3 with N=3. The best fit parameters are presented in Table 1.

The observation of the non-exponential attenuation curves can be explained by making the reasonable assumption that the adsorbate molecules in the intraparticle volume (i.e. in the intraparticle meso- and macropores) and in the interparticle volume (i.e. in large macropores formed by the gaps between the catalyst particles as well as in the liquid on top of the catalyst in the PFG NMR tubes) have different diffusivities. Assuming that there is no or little molecular exchange between different types of pore systems or volumes with different diffusivities, the attenuation curves may be presented as a sum of the exponential terms of the type written in the right part of Eq.1

(2)

where $k=4\gamma^2\delta^2g^2t$, D_i are diffusivities in different types of pore systems of the sample and p_i denotes the probability of finding molecules with the diffusivity D_i. Fitting of the experimental attenuation curves by using Eq.2 has revealed that the smallest number of the exponential terms (viz. N in Eq.2) needed to get a satisfactory agreement between the calculated and the experimental curves is three. Fiq.1 presents the best fit results obtained for N=3 with the best fit parameters shown in Table1. It is seen in Table 1 that the largest diffusivity D_1 is the same for all four catalyst samples. Additional PFG NMR diffusion measurements performed with the PFG NMR tube filled only with liquid 1,3,5 tri-iso-propyl-benzene revealed a diffusivity, which was in an excellent agreement with the value of D_1. This result allows us to assign D_1 to the diffusivity of 1,3,5 tri-iso-propyl-benzene in the interparticle volume of the sample under the conditions that there is no significant molecular exchange with the intraparticle volume and no significant diffusion restrictions imposed by the surface of the particles in the bed. In order to check whether the latter conditions are indeed fulfilled under our measurement conditions we have estimated the root mean square displacement of the probe molecules with the diffusivity D_1 and the diffusion time t=30 ms used in the measurements by applying the Einstein relation $\left\langle r^2 \right\rangle = 6Dt$. This estimate yields the value of $\sqrt{\left\langle r^2 \right\rangle} = 6.4\mu m$, which is much smaller than the mean size of the catalyst particles (~70 μm). Hence, this value is also expected to be much smaller than the mean size of the gaps between the particles in the catalyst samples. This comparison confirms our assignment of D_1.

The second largest fraction of 1,3,5 tri-iso-propyl-benzene in the catalyst samples has diffusivity D_2 (Table 1), which is only slightly smaller than the diffusivity in the liquid phase. Based on the discussion above, this diffusivity can be assigned to the diffusion coefficient in the meso- and macropores of the particles under the condition that there is no or little molecular exchange with the interparticle volume. The fitting results (Table 1) show that in addition to the two fractions of probe molecules discussed above there is an additional, very small fraction with diffusivity $D_{3,}$ which is significantly smaller than D_1 and D_2. The molecules having diffusivity D_3 probably reside in intraparticle mesopores having sizes close to those of the adsorbate molecules. A strong interaction between the pore walls and the molecules, which is expected in this case, can explain low diffusivities. This type of diffusion can be classified as diffusion under molecular confinement. Hence, the formalism of the tortuosity factor is not applicable in this case.

The last column in Table 1 shows the tortuosity factors for the diffusion in the intraparticle meso- and macropores, which were calculated as

$$\eta = \frac{D_1}{D_2}. \qquad (3)$$

Table 1 Best fit parameters obtained by fitting the experimental attenuation curves in Fig.2 by Eq.2 with N=3 and the tortuosity factors for diffusion in the intraparticle meso- and macropores $\eta=D_1/D_2$ for four samples of industrial FCC catalysts.

Catalyst	p_1	$D_1/10^{-10}\mathrm{m^2s^{-1}}$	p_2	$D_2/10^{-10}\mathrm{m^2s^{-1}}$	p_3	$D_3/10^{-11}\mathrm{m^2s^{-1}}$	$\eta=D_1/D_2$
catalyst 1	0.68	2.27	0.3	1.6	0.014	1.2	1.42
catalyst 2	0.63	2.27	0.33	1.36	0.033	1.2	1.67
catalyst 3	0.75	2.27	0.21	1.2	0.02	1.2	1.89
catalyst 4	0.65	2.27	0.30	1.3	0.024	1.2	1.75

These tortuosity factors can be compared with the results of the characterisation of the pore size distribution in the catalyst particles by using mercury porosimetry. The mercury porosimetry measurements have shown the existence of a two distinct types of intraparticle pores: (a) meso- and macropores with sizes smaller than 20 nm, and (b) macropores with a mean size around 100 nm [12]. Table 2 presents the relative volumes of these two types of pores for selected catalyst samples. For comparison, also the data for the specific volume of micropores of zeolite crystals located in the particles are shown.

Table 2. Results of the characterization of intraparticle meso- and macropores by mercury porosimetry and of intracrystalline micropores by nitrogen adsorption for selected industrial FCC catalysts

Catalyst	Specific volume of the meso- and macropores with sizes smaller than 20 nm ($V_{<20\ \mathrm{nm}}$, cm^3/g)	Specific volume of the macropores with sizes in the range of 100 nm ($V_{\sim 100\ \mathrm{nm}}$, cm^3/g)	Specific volume of all intraparticle meso- and macropores ($V_{<20\ \mathrm{nm}} + V_{\sim 100\ \mathrm{nm}}$, cm^3/g)	Specific micropore volume (V_{micro}, cm^3/g)
catalyst 1	0.045	0.211	0.256	0.06
catalyst 3	0.117	0.204	0.321	0.06
catalyst 4	0.105	0.208	0.313	0.06

It is seen that although the total volume of intraparticle pores remains approximately the same in all three catalysts, the fraction of the pores with sizes smaller than 20 nm differs dramatically between different catalysts. Fig.3 shows that there is a correlation between these fractions and the values of the tortuosity factors from Table 2. With increasing fraction of the small (<20 nm) meso- and macropores in the total volume of meso- and macropores the tortuosity factors also increase. This correlation may be intuitively understood by noting that for the same displacements there will be more reflections of the molecules from the pore walls in pore systems with small pores than in those with large pores. Such reflections may lead to an increase of the trajectory lengths, and hence also to an increase of the tortuosity factor.

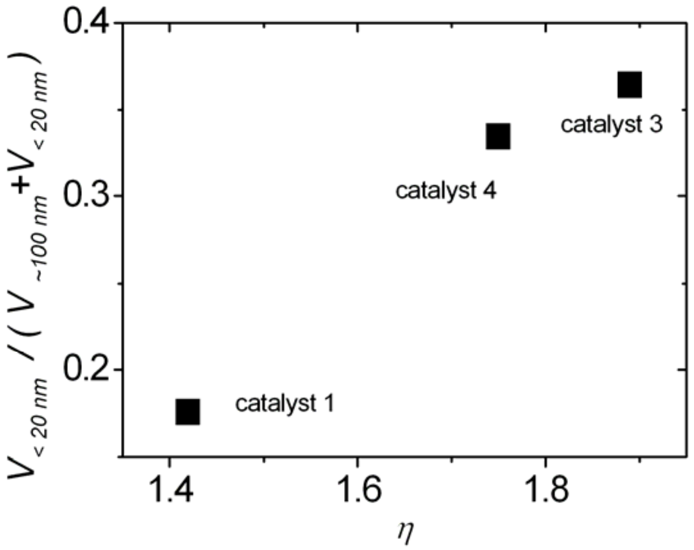

Fig.3 Correlation between the fraction of the intraparticle meso- and macropores with sizes smaller than 20 nm and the tortuosity factors for diffusion of 1,3,5 tri-iso-propyl-benzene in the intraparticle pores

The results in Table 2 show that the micropore volume accounts for less than 20% of the total intraparticle volume. This implies that for the measurements of the tortuosity factors described above it is not essential to use probe molecules with large sizes, which exclude molecular penetration into zeolite micropores. Based on this conclusion we have decided to carry out additional PFG NMR measurements, which are completely analogous to those discussed above, with n-octane used as probe molecules. The size of n-octane molecules is sufficiently small to allow adsorption into micropores of USY zeolite. The results of the PFG NMR diffusion measurements performed with the catalyst samples filled with liquid n-octane were satisfactorily fitted by using Eq.2 with N=3. Using these data the tortuosity factors for diffusion in the intraparticle meso- and macropores were calculated in the same way as it has been done for 1,3,5 tri-iso-propyl-benzene. The values of the tortuosity factors were found to be in a good agreement with the tortuosity factors obtained for 1,3,5 tri-iso-propyl-benzene, despite an order of magnitude difference between the diffusivities of n-octane and of 1,3,5 tri-iso-propyl-benzene in the liquid phase. This confirms that the reported tortuosity factors are correct.

Acknowledgement

This work has been done under coordination of Leipzig University, Germany, in the framework of the “TROCAT” project (contract G5RD-CT-2001-00520), which is funded by the European Community under the “Competitive and Sustainable Growth” Programme.

References

[1] Kärger, J.; Ruthven, D. M. Diffusion in Zeolites and Other Microporous Solids; Wiley & Sons: New York, 1992.

[2] Chen, N. Y.; Degnan, T. F.; Smith, C. M. Molecular Transport and Reaction in Zeolites; VCH: New York, 1994.

[3] Theodorou, D. N.; Snurr, R. Q.; Bell, A. T. Molecular Dynamics and Diffusion in Microporous Materials. In Comprehensive Supramolecular Chemistry; Alberti, G., Bein, T., Eds.; Pergamon Press: Oxford, 1996; pp 507-548.

[4] Kärger, J.; Ruthven, D. M. Self-Diffusion and Diffusive Transport in Zeolite Crystals. In Studies in Surface Science and Catalysis; Elsevier ed.; Chon, H., Ihm, S. K., Uh, Y. S., Eds.; Elsevier: Vol. 105. Amsterdam, 1997; pp 1843-1851.

[5] Auerbach, S. M. Int. Rev. Phys. Chem. 2000, 19, 155-198.

[6] Kärger, J.; Vasenkov, S.; Auerbach, S. Diffusion in Zeolites. In Handbook of Zeolite Science and Technology; Auerbach, S. M., Carrado, K. A., Dutta, P. K., Eds.; Marcel-Dekker Inc.: New York, 2003; pp 341-423.

[7] Callaghan, P. T. Principles of NMR Microscopy; Clarendon Press: Oxford, 1991.

[8] Kimmich, R. NMR Tomography, Diffusometry, Relaxometry; Springer: Berlin, 1997.

[9] Galvosas, P.; Stallmach, F.; Seiffert, G.; Kärger, J.; Kaess, U.; Majer, G. J. Magn. Reson. 2001, 151, 260-268.

[10] Cotts, R. M.; Hoch, M. J. R.; Sun, T.; Markert, J. T. J. Magn. Reson. 1989, 83, 252-266.

[11] Baerlocher, C.; Meier, W. M.; Olson, D. H. Atlas of Zeolite Framework Types, 5 ed.; Elsevier: Amsterdam, 2001.

[12] Kortunov, P.; Vasenkov, S.; Kärger, J.; Fé Elía, M.; Perez, M.; Stöcker, M.; Papadopoulos, G. K.; Theodorou, D.; Drescher, B.; McElhiney, G.; Bernauer, B.; Krystl, V.; Kocirik, M.; Zikanova, A.; Jirglova, H.; Berger, C.; Gläser, R.; Weitkamp, J.; Hansen, E. W. Chem. Mater 2005, submitted.